# THE STRUCTURE OF MELITTIN IN MEMBRANES

HORST VOGEL AND FRITZ JÄHNIG
*Max-Planck-Institut für Biologie, Corrensstr. 38, 7400 Tübingen, Federal Republic of Germany*

ABSTRACT The conformation of the polypeptide melittin in lipid membranes as determined by Raman spectroscopy is a bent $\alpha$-helix formed by the mainly hydrophobic residues 1–21, and a nonhelical COOH-terminal segment of the hydrophilic residues 22–26. Fluorescence quenching experiments on residue Trp19 reveal that all COOH-termini are located on that side of a vesicular membrane to which melittin was added. By means of fluorescence energy transfer between unmodified and modified Trp19 residues, melittin is shown to aggregate in membranes predominantly in the form of tetramers. These and previous results on the location and orientation of melittin permit the development of a model for the structure of melittin tetramers in membranes. The hydrophilic sides of four bilayer-spanning helices face each other to form a hydrophilic pore through the membrane.

## INTRODUCTION

The polypeptide melittin has recently received much attention as a simple model for pore-forming membrane proteins. The molecule is composed of 26 amino acid residues of the following sequence (Habermann and Jentsch, 1967):

Gly Ile Gly Ala Val Leu Lys Val Leu Thr Thr Gly Leu
1 5 10

Pro Ala Leu Ile Ser Trp Ile Lys Arg Lys Arg Gln GlnNH$_2$.
15 20 25

The effect of melittin on membranes ranges from an increase in the permeability for ions (Tosteson and Tosteson, 1981, 1984; Kempf et al., 1982; Hanke et al., 1983) to lysis at high melittin concentration (DeGrado et al., 1982; Hider et al., 1983). The permeability increase is larger for anions than for cations, and larger for monovalent than for divalent cations with no significant difference among the various monovalent cations. In all cases the permeability increases in proportion to the fourth power of the melittin concentration. Furthermore, the permeability increase was found to be voltage dependent as for other polypeptides such as alamethicin. This behavior has led to the notion of "voltage-gated pores." In no case, however, is the molecular structure of such a pore or the molecular mechanism of voltage-gating known.

The structure of melittin has been investigated under various conditions — in crystalline form, dissolved in water or organic solvents, embedded in micelles and in membranes. A variety of experimental techniques have been employed — x-ray diffraction (Terwilliger et al., 1982) NMR (Brown et al., 1982), circular dichroism (CD) (Strom et al., 1978; Dawson et al., 1978; Drake and Hider, 1979; Vogel, 1981; Bello et al., 1982; Knöppel et al., 1982), infrared (IR) (Lavialle et al., 1982; Vogel et al., 1983), fluorescence (Talbot et al., 1979; Georghiou et al., 1982; Quay and Condie, 1983; Quay et al., 1985; Tran and Beddard, 1985), and dielectric relaxation (Sano and Schwarz, 1983).

In the crystal, the conformation of melittin is $\alpha$-helical from the $NH_2$ to the COOH-terminus with a bend of 60° between Thr11 and Gly12. Two pairs of antiparallel helices are mounted crosswise on one another to form a tetramer. In such a structure, elements of a pore are not recognizable.

In water, melittin can exist as a monomer or, at high concentration or high ionic strength, as a tetramer. In the monomeric form, the conformation is disordered, whereas in the tetrameric form it is predominantly $\alpha$-helical. One can assume that the water-dissolved tetramer is essentially the same as the crystalline tetramer, because the crystals were grown from a concentrated aqueous solution of melittin. Whether or not in the water-dissolved tetramer the polar COOH-terminal segments are still $\alpha$-helical as in the crystal has not been clarified. COOH-terminal fragments obtained by protease cleavage were shown to have a high content of $\beta$ structure (Lavialle et al., 1982).

In micelles and membranes, the $\alpha$-helix content is about the same as in the water-dissolved tetramer. NMR measurements on micelle-bound melittin have shown that residues 16–20 are involved in an $\alpha$-helix, the conformation of the neighboring COOH-terminal segment remaining unspecified (Brown et al., 1982). In the same work, circumstantial evidence for a full turn between Thr10 and Pro14 was presented, which would be compatible with the previously proposed wedge-like model for membrane-bound melittin (Dawson et al., 1978). Directly on membrane-bound melittin no data related to the question of a

Horst Vogel's present address is Biozentrum, Universität Basel, CH-4056 Basel, Switzerland

turn are available. A theoretical calculation of the conformation of the $NH_2$-terminal segment of residues 1–20 in an apolar medium predicts a bent $\alpha$-helix as in the crystal (Pincus et al., 1982). When melittin is membrane-bound, the Trp19 residue is located approximately at the height of the C1 atoms of the lipid hydrocarbon chains and the helical segments are oriented at an angle of ~30° relative to the membrane normal (Vogel et al., 1983). If the bend of 60° is preserved, this implies that the bent $\alpha$-helices as a whole are oriented essentially parallel to the membrane normal. Since they consist of ~20 residues, they would just span the bilayer.

Three questions about the structure of melittin in membranes remain open: (*a*) Do the $\alpha$-helices extend up to the COOH-terminus and are they bent as in the crystal or interrupted by a turn to form a wedge-like structure? (*b*) Are the molecules incorporated in a symmetric or asymmetric manner, i.e., do the hydrophilic COOH-termini remain on the same side of the membrane to which melittin was added? (*c*) Do the monomers aggregate and if so, how are they aggregated? We have attempted to answer these questions by performing Raman and fluorescence measurements. Raman spectroscopy was employed to investigate the conformation of melittin in membranes, i.e., to decide whether the COOH-terminal segments are $\alpha$-helical and whether the helices are bent or include a turn. The symmetry of incorporation was studied by fluorescence quenching of Trp19, and the aggregation by fluorescence energy transfer (FET) from Trp19 of native melittin to melittin with a modified Trp19. The results permit the development of a model for the structure of melittin in membranes, in the absence of a membrane potential.

## MATERIALS AND METHODS

### Lipids and Polyglycine

Dimyristoylphosphatidylcholine (DMPC) from Fluka (Neu Ulm, Federal Republic of Germany) was used without further purification. No impurities were detected by thin layer chromatography. Ditetradecylglycerophosphocholine (DPTC) was a gift of Dr. J. Stümpel (Max-Planck-Institut für biophysikalische Chemie, Göttingen, Federal Republic of Germany). The synthesis of this lipid has been described elsewhere (Stümpel, 1982).

Polyglycine was a gift of K. Dornmair (Max-Planck-Institut für Biologie, Tübingen, Federal Republic of Germany) and had an approximate molecular weight of 1,000 corresponding to ~20 residues.

### Purification of Melittin

Melittin from Mack (Illertissen, Federal Republic of Germany) was purified by electrophoresis on cellogel blocks from Serva (Heidelberg, Federal Republic of Germany) in 4 M urea, 0.1 M Tris-acetic acid, pH 7 at 4°C. Melittin was then chromatographed on a column (200 × 2 cm) of Sephadex G75 in 0.1 M ammonium formate buffer, pH 4.5 at 4°C. After freeze drying, melittin was chromatographed on the same column in $10^{-3}$ M HCl in the dark and freeze dried again. Melittin purified by this procedure shows one band after electrophoresis on cellogel strips in 4 M urea, 3 M formic acid, pH 2. No lipid decomposition could be detected in a mixture of $10^{-2}$ M lipid vesicles and $2 \cdot 10^{-4}$ M melittin that have been incubated for 30 h in $10^{-2}$ M Tris buffer, pH 7.4 at 35°C. We therefore consider the purified melittin to be free of phospholipase, which is present in all commercially available melittin preparations.

### Chemical Modification of Melittin

Modified melittin, henceforth called A-melittin, was prepared from native melittin by means of the Koshland reaction using 2-hydroxy-5-nitrobenzylbromide (Serva, Heidelberg, Federal Republic of Germany) as described by Habermann and Kowallek (1970). According to the reaction (Means and Feeney, 1971)

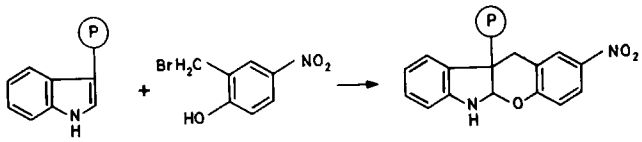


SCHEME I

a nonfluorescent derivative of tryptophan is obtained. In Fig. 1 the absorption spectrum of membrane-bound A-melittin is shown together with the emission spectrum of membrane-bound unmodified melittin. A-melittin was purified twice by chromatography on a column (50 × 2 cm) of Sephadex G25 in $10^{-3}$ M HCl. The yield was 97% as calculated from the absorption spectrum. A-melittin shows the same electrophoretic behavior as melittin on cellogel strips, 4 M urea, 3 M formic acid, pH 2. Its lytic activity is similar to that of native melittin (Habermann and Kowallek, 1970).

### Sample Preparation for Raman Measurements

Melittin used for Raman spectroscopy was further purified by incubation with charcoal to remove fluorescent impurities. The polypeptide was then dissolved at the desired concentration in distilled water. For membrane-bound melittin, $2 \cdot 10^{-2}$ M lipid vesicle suspensions of DTPC in water were prepared by tip sonication for 45 min at 35°C, followed by centrifugation at 12,000 *g* for 10 min at 20°C. Equal volumes of a lipid vesicle suspension and an aqueous melittin solution of appropriate concentration were mixed and incubated at 35°C for 2 h. Subsequently, samples were freeze dried. Water was added to yield a lipid/water weight ratio of 1/2, followed by incubation at 35°C for 2 h. The membrane preparations were transferred to thin-walled glass capillaries, and centrifuged at

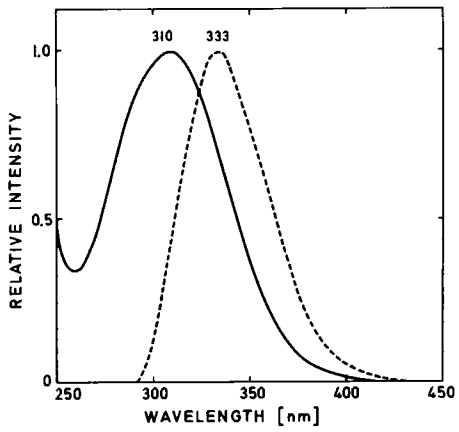


FIGURE 1 Absorption spectrum (—) of A-melittin and fluorescence spectrum (---) of melittin bound to vesicles of DMPC at a molar ratio lipid/melittin = 1/1,000 in $10^{-2}$ M ammonium formate buffer, pH 4.5, at 30°C.

50,000 $g$ for 10 min at 4°C. Pure lipid membranes were prepared identically using water instead of an aqueous melittin solution.

## Raman Measurements

The Raman spectrometer used was described previously (Vogel and Jähnig, 1981). The conditions for measurement were 514.5 nm excitation wave length, 100 mW laser power, and 5 $cm^{-1}$ slit width. For scanning a step size of 0.2 Å and an integration time of 0.5 s per step were chosen. After recording 10 scans in the spectral region of interest, 1 scan at 2,8000–3,400 $cm^{-1}$ was performed.

## Analysis of Raman Data

In the low-frequency range, the Raman spectrum of melittin in water is superimposed on a background that continuously increases with decreasing wave number. This background arises mainly from elastically scattered light which is not rejected by the monochromator, and from low-frequency vibrations of water. We stimulated the background intensity as $I(\nu) = A[\exp(-(\nu - 10)/50) + 0.4\,(10/\nu)^4]$, with $\nu$ in $cm^{-1}$, and $A$ a normalization constant, since the intensity of a pure water sample can be described by such a relation. This intensity was subtracted from the experimental spectrum to obtain the pure spectrum of the polypeptide in this range.

The low-frequency bands of proteins arise from accordion-like vibrations of helical segments. Their frequency is inversely proportional to the length of the helical segments, which, therefore, can be determined. We used Eq. 20 of Peticolas (1979) for this analysis, taking into account that the mean molecular weight per residue is 100, if the helical segments comprise residues 1–21 of melittin.

The amide I band is superimposed upon a weak water band at 1,635 $cm^{-1}$. Therefore, a water spectrum was subtracted from the experimental spectrum, after proper scaling by use of the water band at 3,200 $cm^{-1}$ as an internal standard. Furthermore, a small contribution from lipids was eliminated by subtraction of a lipid spectrum using the lipid band at 2,850 $cm^{-1}$ as an internal standard. This involves an approximation, since the band at 2,850 $cm^{-1}$ changes slightly upon binding of melittin to lipids.

The amide I band arises from a vibration of the peptide bond whose frequency is sensitive to the secondary structure in which the bonds participate. The amide I band can, therefore, be evaluated for the mean secondary structure of the protein. For this analysis we employed the method of Williams (1983). 15 data points are used to describe the measured spectrum between 1,630 and 1,700 $cm^{-1}$. These points are fitted by a superposition of the spectra of 15 reference proteins of known three-dimensional structure. The fit determines the weight of the individual reference proteins in the measured spectrum. Knowing the mean secondary structure of the reference proteins, the mean secondary structure of the protein under study can be derived. Williams distinguished six classes of secondary structure: ordered helix ($O$), disordered helix ($D$), antiparallel strand ($A$), parallel strand ($P$), turn ($T$), and undefined ($U$). The ordered helical structure refers to residues in a helix forming hydrogen bonds to two sides along the helix, the disordered helical structure to residues with <2 hydrogen bonds. Thus, by definition, two residues at each end of a helix belong to the disordered helix class. Proline is attributed to the undefined structure. The spectra of the pure structure classes have been presented by Williams and Dunker (1981). The spectrum of the pure ordered helix class has a maximum at 1,645–1,650 $cm^{-1}$. This case corresponds to infinitely long $\alpha$-helices. With decreasing length of the helices the maximum shifts to higher wave numbers due to the increasing contribution of the disordered helix class. This shift is in agreement with data in the literature (Nevskaya and Chirgadze, 1976).

To fit the measured spectrum by a superposition of reference protein spectra the second method of Williams (1983) was used. Here, the set of reference protein spectra is transformed into a set of orthogonal spectra and a certain number $k_{rank}$ (in the notation of Williams) of them is used for the fit. With increasing $k_{rank}$ the fit becomes better, but the weights of the reference proteins in the fit become less and less reliable and, consequently, the percentages of secondary structure classes become more and more erroneous. A detailed calculation of the error limit leads to an optimal number of $k_{rank} = 7$ for the data of melittin in water, with a maximal error of ±4 in the percentages of secondary structure classes. The magnitude of the error increases with the scatter of the experimental data. This calculation of the error deviates somewhat from the procedure of Williams, and will be presented in a separate communication, but the number $k_{rank} = 7$ lies within the range of values used by Williams.

Two minor modifications of the method of Williams were introduced. (*a*) The protein spectra were normalized in the range 1,630–1,700 $cm^{-1}$. (*b*) The sum of all structure classes for each reference protein were normalized to 100%. This involved the following modifications (Williams' values in parenthesis): For LZM $H_o = 25(24)$; for MEL $H_d = 22(23)$; for BTI $U = 13(14)$; for ConA $H_o = 1(0)$; for INS $H_d = 23(24)$; for ADH $H_o = 19(18)$; for CRA $U = 16(17)$; for fd $H_o = 71(75)$; for PLL $H_o = 66(60)$.

## Sample Preparation for Fluorescence Measurements

A $5 \cdot 10^{-3}$ M suspension of DMPC vesicles in $10^{-2}$ M ammonium formate buffer at pH 4.5 was prepared by tip sonication for 45 min at 30°C, followed by centrifugation for 10 min at 20°C. This buffer was used in all experiments described in this section.

To quench the Trp fluorescence of melittin we used 2,2,6,6-tetramethylpiperidinyl-1-oxycholine (tempocholine) purchased from Molecular Probes (Junction City, OR). 490 μl of a $10^{-3}$ M lipid vesicle suspension and 10 μl of a $5.5 \cdot 10^{-5}$ M melittin solution, both in buffer, were mixed either at 15° or 30°C, and incubated for 30 min at these temperatures. After cooling the one sample from 30° to 15°C, quenching experiments were performed at 15°C by adding appropriate amounts of a $5 \cdot 10^{-2}$ M tempocholine solution in methanol to the vesicle suspensions. In a further series of experiments, after addition of melittin the vesicles were sonicated for 10 min in a bath sonicator, and the quenching experiments carried out as before.

FET measurements between melittin and A-melittin in aqueous solution were performed at low ionic strength (buffer), where melittin is monomeric, and at high ionic strength (buffer, 2 M NaCl), where melittin forms tetramers. Appropriate amounts of a $6.9 \cdot 10^{-5}$ M solution of A-melittin were added to 320 μl of a $10^{-5}$ M melittin solution, both in the corresponding buffers. For FET measurements between melittin and A-melittin in DMPC membranes, appropriate amounts of a $1.66 \cdot 10^{-5}$ M A-melittin solution were added to a vesicle suspension of $4 \cdot 10^{-3}$ M DMPC containing a fixed concentration of melittin, both in buffer, and stored for 30 min at 30°C. Corrections due to light scattering were performed by measuring the scattered light from samples in which melittin was replaced by A-melittin.

## Fluorescence Measurements

The intensity of the Trp fluorescence of melittin was recorded with a Perkin-Elmer MPF-3 spectrometer, exciting at 280 nm and observing at 330 nm. A quartz wedge depolarizer was placed in the emission path to prevent artefacts from polarization. 5 × 5-mm quartz cuvettes were used.

## Evaluation of FET Data

FET between melittin and A-melittin both in aqueous solution and in lipid membranes, can be analyzed to yield the aggregation number, $m$, and the aggregation constant

$$K_m = M_m/(M_1)^m, \qquad (1)$$

with $M_1$ and $M_m$ denoting the numbers of polypeptide monomers and aggregates, respectively. In aqueous solutions $M_1$ and $M_m$ are counted in mol/l, in membranes in particles per lipid molecules. A necessary prerequisite is the construction of structural models for aggregates of

different $m$. Then, the ratio $I/I_0$ of the Trp fluorescence intensities in the presence and absence of $A$-melittin can be expressed as (Veatch and Stryer, 1977)

$$I/I_0 = 1 - \left(\sum_{i=1}^{m-1} D^{m-i} A^i e_i\right)(1 - M_1/M). \quad (2)$$

$D$ and $A$ denote the relative amounts of melittin and A-melittin with $D + A = 1$, and $M$ is the total number of polypeptide molecules. If the number $M_D$ of melittin molecules is given, $M = M_D + M_A = M_D/D$. The $e_i$ are combinations of the FET efficiencies $e_D = 1/(1 + k_D^{-1})$ with $k_D = (R_0/R_{DA})^6$, $R_{DA}$ denoting the distance between a donor and an acceptor, and $R_0^6 = 9.79 \cdot 10^3 \cdot J\kappa^2 Q_0 n^{-4}$. Here, $J$ is the overlap integral of the normalized absorption and emission spectra of the donor and acceptor (Fig. 1). $\kappa^2$ is the orientation factor for dipole-dipole interaction and is assumed to be 2/3 for all donor-acceptor pairs due to the following reasoning. The anisotropy of the Trp fluorescence of membrane-bound melittin was shown to decay to zero on a nanosecond time scale, indicating considerable mobility of the Trp side chains (Georghiou et al., 1982). The same behavior is expected for the modified Trp side chains. Under these conditions, a value of $\kappa = 2/3$ introduces an error of less than ±10% in the FET efficiencies (Kleinfeld, 1985), which is of the same order of magnitude as the error of our experimental data. $Q_0$ is the donor quantum yield in the absence of acceptor and was determined to be 0.23 for the case of monomeric melittin in aqueous solution and 0.36 in membranes. These values were obtained by comparing melittin with L-tryptophan in water whose quantum yield is 0.14 (Eisinger, 1969). $n$ is the refractive index of the milieu assumed to be 1.4 for lipid membranes. For the pair melittin/A-melittin one obtains $R_0 = 29$ Å.

## RESULTS

### Raman Spectroscopy

The Raman spectrum in the range 300–1,700 $cm^{-1}$ and 2,800–3,200 $cm^{-1}$ of tetrameric melittin in water is shown in Fig. 2. The observed Raman bands and their assignments are listed in Table I. The wave numbers of the amide I band, 1,648 $cm^{-1}$, the amide III band, 1,249 $cm^{-1}$, and the amide VI band, 563 $cm^{-1}$, indicate a high $\alpha$-helix content for the structure of tetrameric melittin (Thomas et al., 1983). For the quantitative analysis according to Williams (1983) a 15-point representation of the amide I band is used as shown in Fig. 3. The result for the secondary structure is presented in Table II. Tetrameric melittin in water has an $\alpha$-helix content of 76% corresponding to 20 residues and 8% or 2 residues in each the antiparallel $\beta$-strand, turn, and undefined structure class. The $\alpha$-helix and $\beta$-strand contents are in qualitative agreement with previous results from CD (Bello et al., 1982).

Included in Fig. 3 and Table II are the data for tetrameric melittin in sodium phosphate buffer. With increasing ionic strength the amide I band becomes narrower, indicating a higher $\alpha$-helix content. In 100 mM phosphate buffer the $\alpha$-helix content of melittin reaches 92% corresponding to 24 residues. The negative value for the $\beta$-strand content is an artifact of the analysis in cases of narrow amide I bands. As an example, we studied polyglycine, which shows an even narrower amide I band with a maximum at 1,652 $cm^{-1}$, indicating pure $\alpha$-helix structure (Nevskaya and Chirgadze, 1976). The analysis yields $H_{tot} = 99\%$, $S_{tot} = -15\%$, and $T + U = 16\%$ (Table II). Evidently, this result must be corrected by forcing $S_{tot}$ and $T + U$ toward zero. In the case of melittin in 100 mM phosphate buffer, the analogous correction leads to $S_{tot} = 0$ and $T + U = 8\%$ corresponding to 2 residues.

Fig. 4 $A$ shows the low-frequency spectrum of tetrameric melittin in water. After subtraction of the background (see Materials and Methods), the pure polypeptide spectrum of Fig. 4 $B$ was obtained. Attributing the bands at 34 and 65 $cm^{-1}$ to accordion-like vibrations of $\alpha$-helical segments, the wave numbers can be evaluated for the lengths of the helical segments according to Peticolas (1979). One obtains two segments of 11 and 6 residues.

The amide I region of tetrameric melittin in water (Fig. 2) is shown enlarged in Fig. 5 together with the amide I region of melittin bound to bilayers of DTPC at 15°C. This

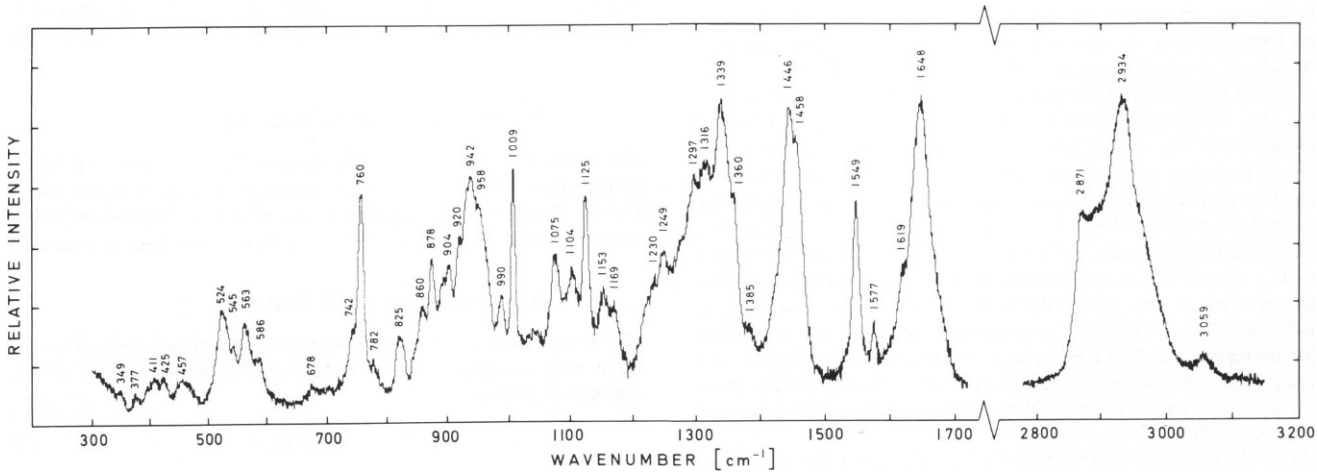


FIGURE 2 Raman spectrum of 2.3 mg melittin dissolved in 10 μl water at 15°C. 36 scans have been summed up in the range 300–1,700 $cm^{-1}$ and 4 scans in the range 2,800–3,200 $cm^{-1}$. The spectrum in the latter range has to be multiplied by a factor of 4.5, to fit into the scale of the 300–1,700-$cm^{-1}$ spectrum. Spectral contributions of water have been subtracted. For comparison, the intensity of the water band at 1,635 $cm^{-1}$ before subtraction was 25% of the intensity of the amide I band at 1,648 $cm^{-1}$.

TABLE I
RAMAN FREQUENCIES OF MELITTIN IN AQUEOUS SOLUTION

| Wave number | Assignment* |
|---|---|
| $cm^{-1}$ | |
| 34 | acoustical modes |
| 65 | |
| 140 | |
| 349 | helix; Gly |
| 377 | $\alpha$-helix; Ala |
| 411 | skeletal |
| 425 | $\alpha$-helix; Val |
| 457 | skeletal; Leu, Ile |
| 524 | $\alpha$-helix; Ala |
| 545 | $\alpha$-helix; Val |
| 563 | amide VI; skeletal; Thr |
| 586 | skeletal; Leu |
| 678 | |
| 742 | |
| 760 | Trp |
| 782 | |
| 825 | |
| 860 | Val |
| 878 | Trp |
| 904 | Ala |
| 920 | Ile, Thr |
| 942 | Val,Leu ($CH_3$, sym. rock in plane) |
| 958 | Val,Leu ($CH_3$, sym. rock out of plane) |
| 990 | Ile |
| 1,009 | Trp |
| 1,075 | |
| 1,104 | Ala |
| 1,125 | Val,Leu,Ile; C–C stretch |
| 1,153 | Val,Leu ($CH_3$, asym. rock in plane) |
| 1,169 | Val,Leu ($CH_3$, asym. rock out of plane) |
| 1,230 | Val |
| 1,249 | amide III |
| 1,297 | $CH_2$ twist/wag |
| 1,316 | |
| 1,339 | |
| 1,360 | Trp |
| 1,385 | $CH_2$ bend |
| 1,446 | |
| 1,458 | |
| 1,549 | Trp |
| 1,577 | |
| 1,619 | |
| 1,648 | amide I |
| 2,871 | C–H stretch |
| 2,934 | |
| 3,059 | |

*According to Thomas et al. (1983).

spectrum has a higher level of noise, because the melittin concentration is ~20 times lower. The difference in concentration was partially compensated by prolonged sampling of data on membrane-bound melittin. Apart from noise, the amide I band of water-dissolved and membrane-bound melittin agree with each other, as is evident from the difference spectrum (Fig. 5). The peak at 1,550 $cm^{-1}$ in the difference spectrum arises from a Trp band and indicates that upon binding of melittin to membranes the

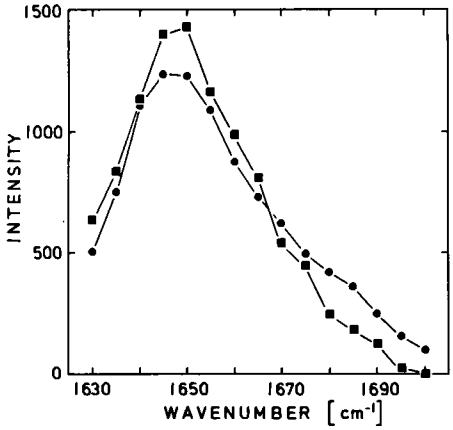


FIGURE 3 15-point representation of the experimental amide I spectrum of tetrameric melittin in water as in Fig. 2 (●) and in 100 mM sodium phosphate buffer, pH 8 (■). The size of the points (●, ■) is a measure of the experimental error, the analytical fit lying within this error.

environment of Trp19 becomes more hydrophobic, as already known from fluorescence studies (Talbot et al., 1979; Vogel, 1981). The identity of the amide I bands of water-dissolved and membrane-bound melittin implies that the secondary structure is very similar in both cases (Table II). This is true irrespective of whether melittin is in an ordered lipid membrane, at 15°C for DTPC, or in a fluid membrane, at 35°C (data not shown). Such constancy of the melittin structure has already been observed in IR studies (Lavialle et al., 1982). Moreover, the $\alpha$-helix content of 76% obtained for membrane-bound melittin is in agreement with previous results from CD (Vogel, 1981) and IR (Lavialle et al., 1982).

## Fluorescence Quenching Measurements

To determine the distribution of COOH-termini between inner and outer bilayer sides we performed fluorescence quenching studies on Trp19, which is located close to the COOH-terminus and accessible from water (Vogel, 1981). As quencher we used tempocholine, which is water-soluble and cannot permeate through membranes in the ordered state (Marsh et al., 1976). Therefore, the quenching experiments were carried out with vesicles of DMPC at 15°C. Melittin was incubated at 15°C with preformed vesicles, at a melittin/lipid ratio low enough so that all melittin molecules bind to the membranes (Vogel, 1981). When tempocholine was added, the Trp fluorescence was quenched as shown by the Stern-Volmer plot of Fig. 6. The quenching efficiency must be compared with that of a second experiment, in which the vesicles with bound melittin were sonicated to produce a symmetric distribution of the COOH-termini, before tempocholine was added. In this case, Trp quenching is only about half as efficient, as seen from Fig. 6. Further sonication after the addition of tempocholine leads to the same quenching efficiency as in the first experiment. Thus, we conclude

TABLE II
SECONDARY STRUCTURE OF MELITTIN IN AQUEOUS SOLUTION AS TETRAMERS AND BOUND TO MEMBRANES OF DTPC, AS DETERMINED FROM THE RAMAN AMIDE I BANDS

| | | *O** | *D* | *A* | *P* | *T* | *U* | $H_{tot}$ | $S_{tot}$ | *T*+*U* |
|---|---|---|---|---|---|---|---|---|---|---|
| Melittin in $H_2O$ and | % | 58.5 | 17.8 | 8.0 | −1.3 | 8.4 | 8.6 | 76.3 | 6.7 | 17.0 |
| bound to membranes | *R* | 15 | 5 | 2 | 0 | 2 | 2 | 20 | 2 | 4 |
| Mellittin in 10 mM Na | % | 60.9 | 25.6 | −0.2 | −1.3 | 7.7 | 7.4 | 86.5 | −1.5 | 15.1 |
| phosphate, pH 7 | *R* | 16 | 6 | 0 | 0 | 2 | 2 | 22 | 0 | 4 |
| Melittin in 100 mM | % | 68.5 | 23.8 | −15.1 | 7.2 | 7.4 | 8.1 | 92.3 | −7.9 | 15.5 |
| Na phosphate, pH8 | *R* | 18 | 6 | − 4 | 2 | 2 | 2 | 24 | −2 | 4 |
| Polyglycine in $H_2O$ | % | 79.0 | 19.8 | −15.0 | 0.2 | 8.1 | 7.9 | 98.8 | −14.8 | 16.0 |

*Abbreviations: *O* = ordered helix, *D* = disordered helix, *A* = antiparallel strand, *P* = parallel strand, *T* = turn, *U* = undefined, $H_{tot} = O + D$, $S_{tot} = A + P$, *R* = number of amino acid residues.
For comparison, the secondary structure of polyglycine in water is included.

that melittin molecules insert into vesicles with their COOH-termini remaining on the outer surface. If melittin and vesicles of DMPC are incubated at 30°C for 30 min before the quenching experiment is performed at 15°C, the same result is found (Fig. 6), which implies that the same insertion also obtains for a fluid membrane. Moreover, the experiments indicate that this asymmetric distribution is stable for at least 1 h. Such an asymmetric insertion of melittin has also been observed in black lipid membranes (Schoch and Sargent, 1980; Kempf et al., 1982).

## Fluorescence Energy Transfer Measurements

To test the efficiency of the donor-acceptor pair melittin and A-melittin, which contains a modified Trp19, we performed FET measurements in aqueous solution at low ionic strength, where melittin is monomeric, and at high ionic strength, where melittin is tetrameric. As expected, at high ionic strength the fluorescence intensity of melittin decreases upon addition of A-melittin, as shown in Fig. 7, whereas at low ionic strength it remains constant.

The data at high ionic strength were further analyzed according to the method of Veatch and Stryer (1977). As discussed in the Introduction, the conformation and aggregation of melittin in water-dissolved tetramers is similar to that in crystalline tetramers. In the crystal structure, each Trp19 has one neighbor at a distance of 7 Å and two at 26 Å (Terwilliger et al., 1982). With these values for the donor-acceptor distances $R_{DA}$, the best fit of Eq. 2 to the data of Fig. 7 is obtained with $K_4 = 1 \cdot 10^{-15}\ M^{-3}$. This value is in fairly good agreement with the value $K_4 = 4 \cdot 10^{-13}\ M^{-3}$ (at pH 5.4) derived by Quay and Condie (1982)

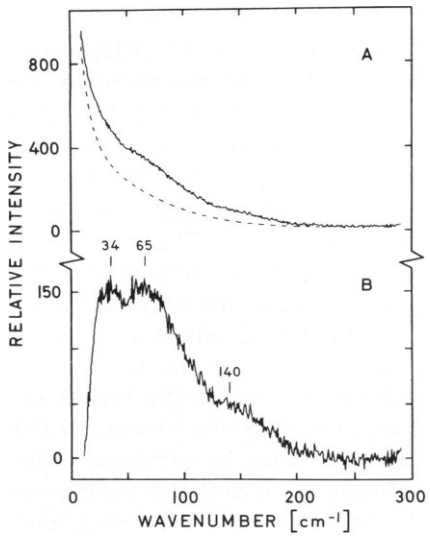


FIGURE 4 (*A*) Low-frequency Raman spectrum of 10 mg melittin in 10 μl water at 15°C. 6 scans have been summed. The dashed curve represents a calculated background contribution (see Materials and Methods). (*B*) Difference between the experimental spectrum and the calculated background in *A*.

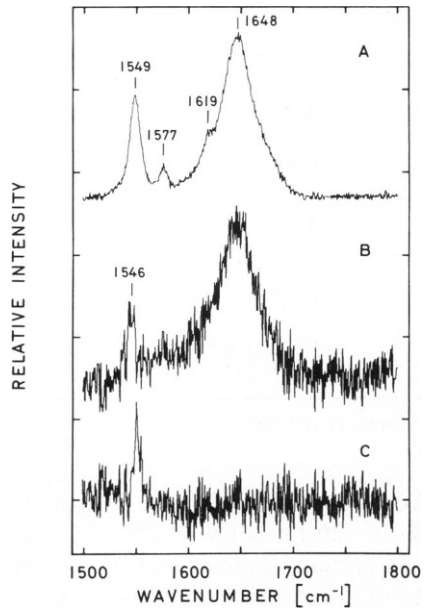


FIGURE 5 Raman spectra in the amide I region at 15°C. (*A*) Melittin in water as in Fig. 2. (*B*) Melittin in DTPC membranes at a molar ratio lipid/melittin = 100. 432 scans have been summed up. Spectral contributions of water and lipids have been subtracted. (*C*) Difference spectrum *A*–*B*.

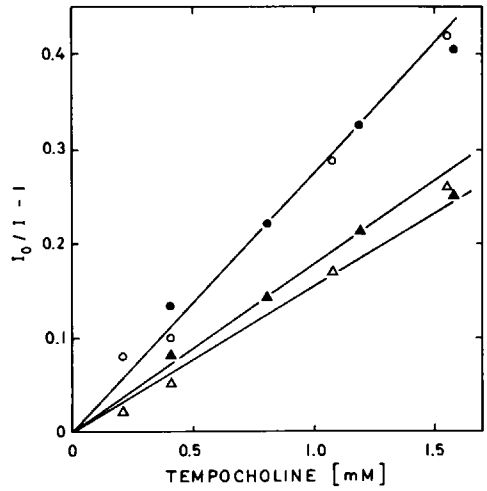


FIGURE 6 Stern-Volmer plot of the Trp fluorescence of melittin in DMPC membrane vesicles at a molar ratio lipid/melittin = 890 at different concentrations of tempocholine. $I_0$ and $I$ are the fluorescence intensities at 330 nm in the absence and in the presence of tempocholine, respectively. Titration with tempocholine was performed at 15°C after adding melittin to the vesicle suspension at 30°C (*full symbols*) and 15°C (*open symbols*), with sonication (▲, △) and without sonication (●, ○) of the sample.

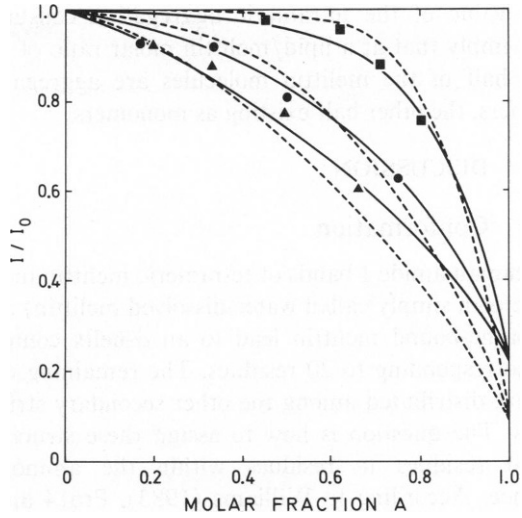


FIGURE 8 Concentration dependence of FET between donor melittin and acceptor A-melittin in membranes of DMPC at 30°C. The relative fluorescence intensity $I/I_0$ is plotted against the molar fraction $A$ of A-melittin for different values of the molar ratio of melittin to lipid $M_D$ = 1/9,410 (■), 1/3,855 (●), and 1/2,350 (▲). The curves represent fits according to Eq. 2 with $m = 4$, $K_4 = 2.1 \cdot 10^9$ (—), and $m = 6$, $K_6 = 3.4 \cdot 10^{15}$ (---).

from the shift of the Trp fluorescence maximum upon aggregation. Thus, our donor-acceptor pair is well suited for studying melittin aggregation.

To investigate the aggregation of melittin in membranes, A-melittin was added to vesicles of DMPC containing melittin. As shown in Fig. 8 for 30°C, the Trp fluorescence intensity decreases. Since the molar ratio lipid/total melittin was 1,000 or higher, FET would be ineffective for homogeneously distributed monomers (Estep and Thompson, 1979), so that melittin must be partially aggregated. Furthermore, the efficiency of FET significantly increases with increasing melittin content (Fig. 8), hence the monomer-oligomer equilibrium is shifted to the side of the oligomers with increasing melittin concentration.

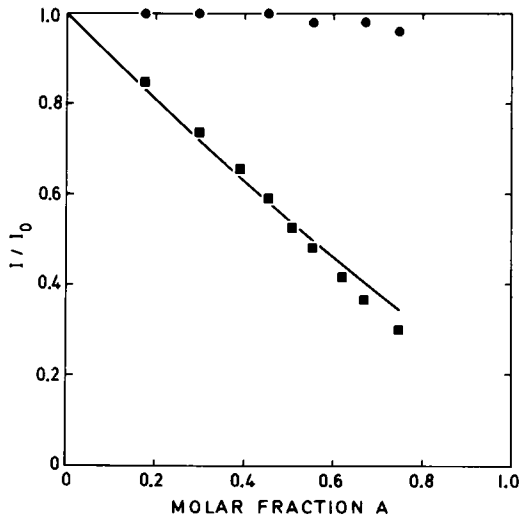


FIGURE 7 Concentration dependence of FET between donor melittin and acceptor A-melittin in ammonium formate buffer, pH 4.5, at 25°C. The relative fluorescence intensity $I/I_0$ is plotted against the molar fraction $A$ of A-melittin for the case of low ionic strength (buffer) (●) and high ionic strength (buffer, 2 M NaCl) (■). The straight line represents a fit according to Eq. 2 with $K_4 = 1 \cdot 10^{15}\ M^{-3}$.

The dependence of FET on both the donor and the acceptor concentrations was analyzed again by the method of Veatch and Stryer (1977). Since in this case the structure of the aggregates is not known, the strategy was to assume different structures and to compare them in their ability to fit the data. First, we assumed aggregation in a tetramer, because conductivity measurements provided evidence for a tetramer as the conducting unit (Tosteson and Tosteson, 1981). The monomers were assumed to be bent $\alpha$-helices oriented parallel to the membrane normal with their COOH-termini all on the same side of the membrane. Four of them were placed on a ring with the Trp residues facing the surrounding lipids (Fig. 10). Each Trp residue then has one neighbor at a distance of 30 Å and two at a distance of $30/\sqrt{2}$ Å = 21 Å. Under these assumptions, the FET data could well be fitted (Fig. 8) with an aggregation constant of $K_4 = 2.1 \cdot 10^9$. For comparison, the data were also fitted assuming $m = 2$ and $m = 6$ with the monomer conformation and orientation unaltered. In the case $m = 2$, each Trp residue has one neighbor at a distance of 30 Å. For $m = 6$, the radius of the ring on which the monomers are located is increased, each Trp residue has one neighbor at a distance of 42 Å, two at $42\sqrt{3}/2$ Å = 36 Å, and two at 42/2 Å = 21 Å. For both dimeric and hexameric aggregation, the fits were poorer than for tetrameric aggregation (Fig. 8). The

above value of the tetrameric aggregation constant $K_4$ would imply that at a lipid/melittin molar ratio of 1,000, about half of the melittin molecules are aggregated in tetramers, the other half existing as monomers.

## DISCUSSION

### Conformation

The Raman amide I bands of tetrameric melittin in water (henceforth simply called water-dissolved melittin) and of membrane-bound melittin lead to an $\alpha$-helix content of 76% corresponding to 20 residues. The remaining 6 residues are distributed among the other secondary structure classes. The question is how to assign these structurally defined residues to residues within the amino acid sequence. According to Williams (1983), Pro14 and the amidated Gln26 belong to the undefined structure class. For the remaining 4 nonhelical residues (2*A* and 2*T*) two possibilities may be envisioned. They may be assigned either to the polar COOH-terminal segment yielding a more or less disordered COOH-terminus, or to the region between Thr10 and Pro14, yielding a turn as required in the wedge-like model for melittin. To decide between these two possibilities, the secondary structure of melittin at increasing ionic strength was investigated. The idea was that if ionic strength affects the conformation of melittin, it acts on the conformation of the COOH-terminal segment that bears four positive charges. In analogy to polylysine (Carrier and Pézolet, 1984), one would expect that upon shielding of the charges at high ionic strength, the COOH-terminal segment adopts an ordered structure, i.e., becomes $\alpha$-helical. The experiments were performed on melittin in aqueous solution, but their result should also be applicable to membrane-bound melittin, because the polar COOH-terminal segment is supposed not to enter the membrane but to remain in contact with water. The result was, indeed, that with increasing ionic strength the $\alpha$-helix content increases reaching 92% or 24 residues (Table II). This is the maximally possible $\alpha$-helix content, since Pro14 and Gln26 remain member of the undefined structure class. Hence, the ionic strength effect provides evidence that the four nonhelical residues found for melittin in pure water belong to the polar COOH-terminal segment.[1] As a consequence, the 20 helical residues must then be assigned to the $NH_2$-terminal segment of residues 1–21 (Table III). Lys 21 is a good candidate for the helix to end, because Lys has a preference for the COOH-terminal end of helices (Chou and Fasman, 1978).

The melittin helix cannot be completely regular, since Pro14 is located in the helical region. This is demonstrated by two further experimental results. The analysis of the amide I band yields 5–6 residues in the disordered helix class. This is more than the four disordered residues required for one regular helix (Williams, 1983). Hence, the melittin helix should have some internal disorder. Secondly, from the low-frequency spectrum of melittin two helical segments were obtained, 6 and 11 residues long. Since a turn in the melittin helix has already been excluded by the ionic strength effect, the sole possibility for internal disorder is a bend. Thus, our experimental results tend to indicate that the helix of water-dissolved and membrane-bound melittin is essentially the same as in the crystal, apart from the COOH-terminus. This leads to the model for the conformation of melittin in water and membranes as shown in Fig. 9.

TABLE III
PROPOSED ASSIGNMENTS OF SECONDARY STRUCTURE CLASSES TO AMINO ACID RESIDUES FOR MELITTIN IN AQUEOUS SOLUTION AS TETRAMERS AND BOUND TO MEMBRANES

| sequence* | GIGAV | LKVLT | TGLPA | LISWI | KRKRQ | Q |
|---|---|---|---|---|---|---|
| Tetramers in $H_2O$ and membrane-bound | *DDOOO* | *OOOOD* | *OOOUO* | *OOOOD* | *DATTA*‡ | *U* |
| Tetramers in 10 mM Na phosphate, pH 7 | *DDOOO* | *OOOOD* | *OOOUO* | *OOOOO* | *ODDTT* | *U* |
| Tetramers in 100 mM Na phosphate, pH 8 | *DDOOO* | *OOOOD* | *OOOUO* | *OOOOO* | *OODD* | *U* |

*In one-letter code for amino acid residues.
‡The structure classes in the segment ATTA may be interchanged.

### Orientation and Aggregation

In previous fluorescence quenching experiments employing lipid-soluble quenchers we found that Trp19 is located at about the height of the C1 atoms of the lipid hydrocarbon chains (Vogel, 1981). IR spectroscopy on oriented membranes revealed that the two $\alpha$-helical segments of the bent $\alpha$-helices are oriented essentially parallel to the membrane normal (Vogel et al., 1983).[2] This implies that the bent $\alpha$-helix is incorporated into membranes in a bilayer-spanning manner. What remains to be specified is the symmetry of the incorporation. The fluorescence quenching experiments on Trp19 employing a water-soluble quencher led to the result that all hydrophilic COOH-termini remain on that side of the membrane to which they were added, at least for 1 h.

[1]Indirect evidence for a disordered structure of the COOH-terminus is provided by monoclonal antibodies against melittin (King et al., 1984). The major antigenic determinant of melittin is located in the COOH-terminal segment. In general, antigenic determinants of proteins are regions of low order and high mobility (Westhof et al., 1984), hence, the COOH-terminal segment should be disordered.

[2]These IR measurements were carried out on membranes of DTPC or DMPC and melittin in the ordered lipid phase. Since then, the experiments have been extended to the fluid phase employing CD, and the results are in agreement with the IR data (H. Vogel, unpublished).

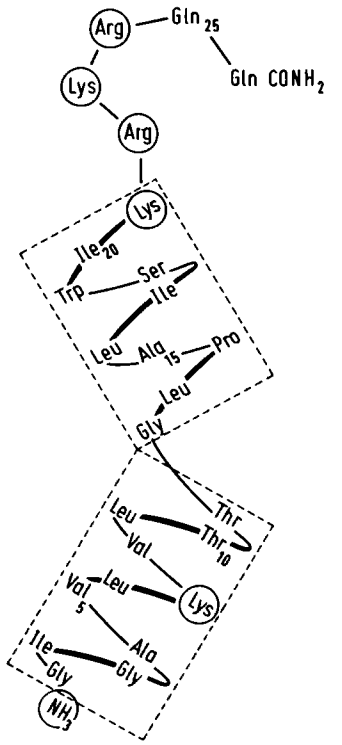


FIGURE 9 Schematic model of the conformation of water-dissolved and membrane-bound melittin. Two $\alpha$-helical segments of residues 1–11 and 12–21 are bent by 60° relative to each other, the COOH-terminal segment of residues 22–26 being nonhelical. The convex side of the bent helix is hydrophilic, the concave side hydrophobic. Circles denote positively charged residues.

If melittin molecules are incorporated into membranes in this way, a final problem arises. Inspection of the bent helix in Fig. 9 reveals that it is hydrophobic only on one side, the concave side, whereas the other side is hydrophilic due to the side groups of Lys7, Thr10, Thr11, Ser18, and Lys21, and the nonhydrogen-bonded NH and C=O backbone groups at the bend. Such a helix has been called "amphipathic" (Eisenberg et al., 1982). Upon insertion into a membrane with the average helix axis parallel to the membrane normal, the hydrophilic side makes contact with the hydrophobic chains of the lipids, which is energetically unfavorable. To avoid this contact several helices may aggregate with their hydrophilic sides facing each other. Indeed, measurement of FET between melittin and melittin modified at the Trp19 residue indicated partial aggregation of melittin in membranes. Assuming the conformation, position, and orientation of the melittin molecules as discussed above, the best fit to the data was obtained for aggregation in the form of tetramers. Evidence for tetrameric aggregation of melittin has already been provided by conductivity measurements on black lipid membranes which showed an increase of the conductivity with the fourth power of the melittin concentration (Tosteson and Tosteson, 1981). Our FET measurements lend further support to the tetrameric aggregation of melittin in membranes.

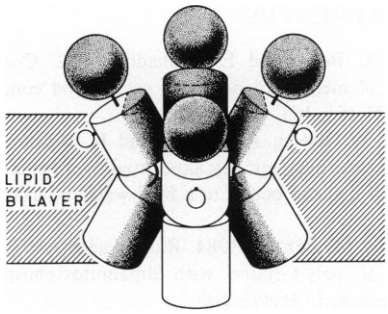


FIGURE 10 Schematic model of tetrameric melittin in membranes. Spheres represent the nonhelical COOH-terminal segments of melittin, cylinders the membrane-bound $\alpha$-helical segments with the hydrophobic sides (*white*) facing the bilayer lipids and the hydrophilic sides (*dotted*) facing each other, thus forming a bilayer-spanning polar pore. The Trp residues are shown to illustrate the position of fluorescence donors and acceptors.

A model for membrane-bound melittin which is compatible with all our experimental results is presented in Fig. 10. The orientation of the two helical segments may as well be less symmetric, the upper segment of residues 12–21 may be more tilted to increase the distance between the charged COOH-terminal segments. This would bring the $NH_2$-terminal segments of residues 1–11 in a more parallel orientation. Furthermore, the aggregate may be shifted upwards or downwards, but only by a few angstroms, because otherwise the hydrophobic sides of the helices would no longer contact the hydrophobic lipid chains.

It is instructive to compare the aggregation of melittin in membranes and in water or the crystal. The kind of aggregation seems to be completely different, although the conformations of the monomers are essentially the same. In water, the hydrophobic sides of the helices associate to avoid contact with the surrounding water — in membranes, the hydrophilic sides of the helices face each other to avoid contact with the surrounding lipid chains. Thus, one structure is the inside-out version of the other.

The model for melittin in membranes as shown in Fig. 10 intuitively gives the impression of a pore. The hydrophilic sides of the four helices form a polar surface through the membrane, probably covered with water, along which polar molecules can diffuse. Indeed, melittin functions as a pore and by neutron scattering water molecules were detected up to the middle of bilayers that contained melittin (Strom et al., 1983). Furthermore, the model bears many analogies to that proposed for alamethicin by Fox and Richards (1981). Many of their ideas about opening and closing of a pore might be adapted to melittin. However, the experimental investigation of the structure of melittin under the action of a membrane potential must await future work.

We thank K. Dornmair for the gift of polyglycine and for many helpful discussions.

*Received for publication 21 February 1985 and in final form 24 February 1986.*

## REFERENCES


Bello, J., H. R. Bello, and E. Granados. 1982. Conformation and aggregation of melittin: dependence on pH and concentration. *Biochemistry.* 21:461–465.

Brown, L. R., W. Braun, A. Kumar, and K. Wüthrich. 1982. High resolution nuclear magnetic resonance studies of the conformation and orientation of melittin bound to a lipid-water interface. *Biophys. J.* 37:319–328.

Carrier, D., and M. Pézolet. 1984. Raman spectroscopic study of the interaction of poly-L-lysine with dipalmitoylphosphatidylglycerol bilayers. *Biophys. J.* 46:497–506.

Chou, P. Y., and G. D. Fasman. 1978. Empirical predictions of protein conformation. *Annu. Rev. Biochem.* 47:251–276.

Dawson, C. R., A. F. Drake, J. Helliwell, and R. C. Hider. 1978. The interaction of bee melittin with lipid bilayer membranes. *Biochim. Biophys. Acta.* 510:75–86.

DeGrado, W. F., G. F. Musso, M. Lieber, E. T. Kaiser, and F. J. Kézdy. 1982. Kinetics and mechanism of hemolysis induced by melittin and by a synthetic melittin analogue. *Biophys. J.* 37:329–338.

Drake, A. F., and R. C. Hider. 1979. The structure of melittin in lipid bilayer membranes. *Biochim. Biophys. Acta.* 555:371–373.

Eisenberg, D., R. M. Weiss, and T. C. Terwilliger. 1982. The helical hydrophobic moment: a measure of the amphiphilicity of a helix. *Nature (Lond.).* 299:371–374.

Eisinger, J. 1969. A variable temperature, U.V. luminescence spectrograph for small samples. *Photochem. Photobiol.* 9:247–258.

Estep, T. N., and T. E. Thompson. 1979. Energy transfer in lipid bilayers. *Biophys. J.* 26:195–208.

Fox, R. O., and F. M. Richards. 1982. A voltage-gated ion channel model inferred from the crystal structure of alamethicin at 1.5 Å resolution. *Nature (Lond.).* 300:325–330.

Georghiou, S., M. Thompson, and A. K. Mukhopadhyay. 1982. Melittin-phospholipid interaction studied by employing the single tryptophan residue as an intrinsic fluorescent probe. *Biochim. Biophys. Acta.* 688:441–452.

Habermann, E., and J. Jentsch. 1967. Sequenzanalyse des Melittins aus den tryptischen und peptischen Spaltstücken. *Hoppe Seyler's Z. Physiol. Chem.* 348:37–50.

Habermann, E., and H. Kowallek. 1970. Modifikation der Aminogruppen und des Tryptophans in Melittin als Mittel zur Erkennung der Struktur-Wirkungs-Beziehung. *Hoppe Seyler's Z. Physiol. Chem.* 351:884–890.

Hanke, W., C. Methfessel, H. U. Wilmsen, E. Katz, G. Jung, and G. Boheim. 1983. Melittin and a chemically modified trichotoxin form alamethicin-type multi-state pores. *Biochim. Biophys. Acta.* 727:108–114.

Hider, R. C., F. Khader, and A. S. Tatham. 1983. Lytic activity of monomeric and oligomeric melittin. *Biochim. Biophys. Acta.* 728:206–214.

Kempf, C., R. D. Klausner, J. N. Weinstein, J. Van Renswoude, M. R. Pincus, and R. Blumenthal. 1982. Voltage-dependent trans-bilayer orientation of melittin. *J. Biol. Chem.* 257:2469–2476.

King, T. P., L. Kochoumian, and A. Joslyn. 1984. Melittin-specific monoclonal and polyclonal IgE and $IgG_1$ antibodies from mice. *J. Immunol.* 133:2668–2673.

Kleinfeld, A. M. 1985. Tryptophan imaging of membrane proteins. *Biochemistry.* 24:1874–1882.

Knöppel, E., D. Eisenberg, and W. Wickner. 1979. Interactions of melittin, a preprotein model, with detergents. *Biochemistry.* 18:4177–4181.

Lavialle, F., R. G. Adams, and I. W. Levin. 1982. Infrared spectroscopic study of the secondary structure of melittin in water, 2-chloroethanol, and phospholipid bilayer dispersions. *Biochemistry.* 21:2305–2312.

Marsh, D., A. Watts, and P. F. Knowles. 1976. Evidence for phase boundary lipid. Permeability of tempocholine into dimyristoylphosphatidylcholine vesicles at the phase transition. *Biochemistry.* 15:3570–3578.

Means, G. E., and R. E. Feeney. 1971. Chemical modification of proteins. Holden-Day, San Francisco.

Nevskaya, N. A., and Y. N. Chirgadze. 1976. Infrared spectra and resonance interactions of amide-I and II vibrations of α-helix. *Biopolymers.* 15:637–648.

Peticolas, W. L. 1979. Mean-square amplitudes of the longitudinal vibrations of helical polymers. *Biopolymers.* 18:747–755.

Pincus, M. R., R. D. Klausner, and H. A. Scheraga. 1982. Calculation of the three-dimensional structure of the membrane-bound portion of melittin from its amino acid sequence. *Proc. Natl. Acad. Sci. USA.* 79:5107–5110.

Quay, S. C., and C. C. Condie. 1983. Conformational studies of aqueous melittin: thermodynamic parameters of the monomer-tetramer self-association reaction. *Biochemistry.* 22:695–700.

Quay, S. C., C. C. Condie, and K. W. Minton. 1985. Conformational studies of aqueous melittin: collisional quenching of tryptophan-19 fluorescence in melittin. *Biochim. Biophys. Acta.* 831:22–29.

Sano, T., and G. Schwarz. 1983. Structure and dipole moment of melittin molecules in butanol/water as derived from dielectric dispersion and circular dichroism. *Biochim. Biophys. Acta.* 745:189–193.

Schoch, P., and D. F. Sargent. 1980. Quantitative analysis of the binding of melittin to planar lipid bilayers allowing for the discrete-charge effect. *Biochim. Biophys. Acta.* 602:234–247.

Strom, R., C. Crifo, V. Viti, L. Guidoni, and F. Podo. 1978. Variations in circular dichroism and proton-NMR relaxation properties of melittin upon interaction with phospholipids. *FEBS (Fed. Eur. Biochem. Soc.) Lett.* 96:45–50.

Strom, R., F. Podo, C. Crifo, C. Berthet, M. Zulauf, and G. Zaccai. 1983. Structural aspects of the interaction of bee venom peptide melittin with phospholipids. *Biopolymers.* 22:391–397.

Stümpel, J. 1982. Kalorimetrie und Röntgenstrukturanalyse an Lecithin-Modellmembranen. Dissertation, Universität Braunschweig.

Talbot, J. C., J. Dufourcq, J. DeBony, J. F. Faucon, and C. Lussan. 1979. Conformational change and self-association of monomer melittin. *FEBS (Fed. Eur. Biochem. Soc.) Lett.* 102:191–193.

Terwilliger, T. C., L. Weissman, and D. Eisenberg. 1982. The structure of melittin in the form I crystals and its implication for melittin's lytic and surface activities. *Biophys. J.* 37:353–361.

Thomas, G. J., B. Prescott, and L. A. Day. 1983. Structure similarity, difference and variability in the filamentous viruses fd, If1, Ike, Pf1, Xf, and Pf3. *J. Mol. Biol.* 165:321–356.

Tosteson, M. T., and D. C. Tosteson. 1981. The sting. Melittin forms channels in lipid bilayers. *Biophys. J.* 36:109–116.

Tosteson, M. T., and D. C. Tosteson. 1984. Activation and inactivation of melittin channels. *Biophys. J.* 45:112–114.

Tran, C. D., and G. S. Beddard. 1985. Studies of the fluorescence from tryptophan in melittin. *Eur. Biophys. J.* 13:59–64.

Veatch, W., and L. Stryer. 1977. The dimeric nature of the gramicidin A transmembrane channel: conductance and fluorescence energy transfer studies of hybrid channels. *J. Mol. Biol.* 113:89–102.

Vogel, H. 1981. Incorporation of melittin into phosphatidylcholine bilayers. Study of binding and conformational changes. *FEBS (Fed. Eur. Biochem. Soc.) Lett.* 134:37–42.

Vogel, H., and F. Jähnig. 1981. Conformational order of the hydrocarbon chains in lipid bilayers. A Raman spectroscopic study. *Chem. Phys. Lipids.* 29:83–101.

Vogel, H., F. Jähnig, V. Hoffmann, and J. Stümpel. 1983. The orientation of melittin in lipid membranes. A polarized infrared spectroscopic study. *Biochim. Biophys. Acta.* 733:201–209.

Westhof, E., D. Altschuh, D. Moras, A. C. Bloomer, A. Mondragon, A. Klug, and M. H. V. Van Regenmortel. 1984. Correlation between segmental mobility and the location of antigenic determinants in proteins. *Nature (Lond.).* 311:123–126.

Williams, R. W. 1983. Estimation of protein secondary structure from the laser Raman amide I spectrum. *J. Mol. Biol.* 166:581–603.

Williams, R. W., and A. K. Dunker. 1981. Determination of the secondary structure of proteins from the amide I band of the laser Raman spectrum. *J. Mol. Biol.* 152:783–813.